

Electronic Supplementary Information (ESI)

Synthesis of Mordenite Nanosheets with Shortened Micropore Channel Length and Enhanced Catalytic Activity

Meng Ma,^{ab} Xiumin Huang,^a Ensheng Zhan,^a Yan Zhou,^a Huifu Xue^a and Wenjie Shen^{*a}

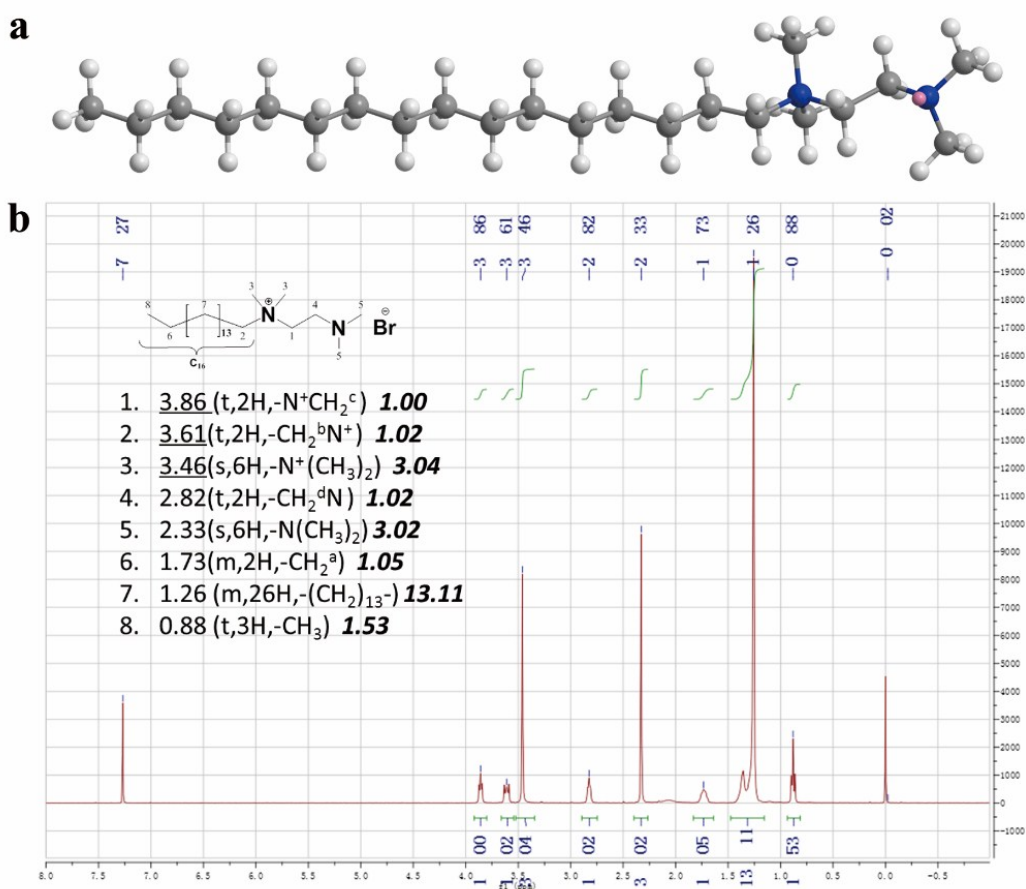
^aState Key Laboratory of Catalysis, Dalian Institute of Chemical Physics, Chinese Academy of
Sciences, Dalian 116023, China

^bUniversity of Chinese Academy of Sciences, Beijing 100049, China

*Corresponding author. E-mail: shen98@dicp.ac.cn

1. Synthesis of the structure-directing agent

$C_{16}H_{33}-N^+(CH_3)_2-C_2H_4-N(CH_3)_2Br$ (C_{16-2-0}) was prepared as the structure-directing agent (SDA). 0.04 mol 1-bromocetane (97%, Aldrich) and 0.40 mol N,N,N',N'-tetramethyl-1,2-diaminoethane (99%, Sigma-Aldrich) were dissolved in 120 ml acetonitrile/toluene (1:1 vol./vol.), and the mixture was heated to 333 K and kept for 10 h. After cooling down to room temperature naturally, the solution was stored in a refrigerator overnight, filtered and washed with cold diethyl ether. The resulting solid was dried under vacuum and at room temperature overnight. 1H NMR analysis has identified the product as $C_{16}H_{33}-N^+(CH_3)_2-C_2H_4-N(CH_3)_2Br$.



Chem3D structure (a) and (b) 1H NMR spectrum of C_{16-2-0} .

2. Synthesis of the MOR nanosheets

MOR nanosheets were hydrothermally synthesized by using C_{16-2-0} as the SDA. In a typical procedure, 12.26 g tetraethylorthosilicate (TEOS, Si content was 28.4% in the form of SiO_2 , Sinopharm Chemical Reagent), 1.30 g $Al_2(SO_4)_3 \cdot 18H_2O$ (99%, Tianjin Kemiou Chemical Reagent), 1.35 g NaOH (96%, Sinopharm Chemical Reagent), 0.98 g C_{16-2-0} , and 45.11g distilled water were mixed, forming a white gel with a molar composition of 8.4 $Na_2O:1.0$

Al_2O_3 :30 SiO_2 :1260 H_2O :120 EtOH:1.2 C_{16-2-0} . The ethanol (“120 EtOH” in the synthesis composition) was generated by TEOS hydrolysis. The resulting mixture was stirred at room temperature for 24 h, and then transferred into a Teflon-lined stainless-steel autoclave. The autoclave was heated to 423 K and maintained at that temperature under tumbling conditions for 6 days. The solid product was collected by filtration, thoroughly washed with distilled water, dried at 383 K overnight, and finally calcined at 823 K in air for 8 h.

To prepare the HMOR catalyst, the as-synthesized zeolite was ion-exchanged with a 1.0 mol/L NH_4NO_3 aqueous solution at 353 K for 12 h. After repeating such a procedure for three times, the sample was dried at 383 K overnight and calcinated at 773 K for 6 h in air, yielding HMOR nanosheets. For comparison, a commercial Na-mordenite ($\text{SiO}_2/\text{Al}_2\text{O}_3=18$, Dalian Hongda Chemicals) was ion-exchanged as the above procedure. For keeping a similar $\text{SiO}_2/\text{Al}_2\text{O}_3$ ratio, the dried commercial H-mordenite was treated with HNO_3 solution (4.0 mol/L) at 373 K for 10 h and calcined at 773 K for 6 h in air.

3. Characterization

Powder X-ray diffraction (XRD) patterns were recorded on a D/MAX 2500/PC diffractometer (Rigaku, Japan) using a $\text{Cu K}\alpha$ ($\lambda=0.154$ nm) radiation source that was operated at 40 kV and 200 mA.

Field-emission scanning electron microscopy (FESEM) images were taken on a Philips FEI Quanta 200F microscope operated at 20 kV or a JEOL JSM-7800F microscope at 1 kV. Transmission electron microscopy (TEM) analysis was performed on a JEOL JEM-2100 operated at 200 kV.

Nitrogen adsorption-desorption isotherms were recorded on a Quantachrome Autosorb-1-MP adsorption analyzer at 77 K. Prior to the measurement, the samples were outgassed at 573 K for 5 h. The total surface area was obtained from the BET (Brunauer-Emmet-Teller) equation from the adsorption isotherms at P/P_0 between 0.005 and 0.05, and the total pore volume was calculated from the adsorption isotherms at $P/P_0 = 0.99$. The micropore surface areas and volumes were calculated using the t-plot method. The micropore size distributions were calculated by the HK (Horvath-Kawazoe) (micropores) method from the adsorption branches of the isotherms.

Solid-state magic-angle-spinning (MAS) nuclear magnetic resonance (NMR) experiments were conducted on a Varian Infinityplus-400 spectrometer. ^{29}Si MAS NMR spectra were obtained at 79.4 MHz using 7.5-mm MAS probe with a spinning rate of 10 kHz. The chemical shifts were referenced to *DSS* (4,4-dimethyl-4-silapentane-1-sulfonic acid). ^{27}Al MAS NMR

spectra were recorded at a resonance frequency of 104.2 MHz with a spinning rate of 10 kHz, and the chemical shifts were referenced to $(\text{NH}_4)\text{Al}(\text{SO}_4)_2 \cdot 12\text{H}_2\text{O}$ at -0.4 ppm.

Temperature-programmed desorption of ammonia (NH_3 -TPD) experiments were conducted with a U-shape quartz tube reactor. 100-mg sample was heated to 773 K at a rate of 5 K/min and maintained at this temperature for 1 h under He flow (30 mL/min). After cooling down to 473 K, the sample was purged with a 10 vol. % NH_3/He mixture (30 mL/min) for 30 min. The physically adsorbed ammonia was removed by purging the sample with a 0.6 vol % $\text{H}_2\text{O}/\text{He}$ mixture (30 mL/min) at 473 K for 1 h. Desorption of ammonia was then performed by heating the sample to 923 K at a rate of 10 K/min under He flow (30 mL/min), and the amount of NH_3 desorbed was monitored by a mass spectrometry (Omnistar QMS200). The amounts of the acid sites in the 12-MR and 8-MR pores (8-MR channel and side-pockets) was measured by an approach using pre-adsorption of pyridine on the HMOR samples, as we previously described.^{1, 2}

4. Catalytic reaction

DME carbonylation was carried out on a continuous flow fixed-bed reactor (i.d. 8 mm). 300 mg catalysts (40–60 mesh) was loaded into the reactor and treated with N_2 (30 mL/min) at 773 K for 1 h. After cooling down to 473 K, a mixture of 5 vol.% DME/50 vol.% $\text{CO}/2.5$ vol.% $\text{N}_2/42.5$ vol.% He was introduced through a mass-flow controller (6.25 mL/min) and the reactor was pressurized to 1.0 MPa. The effluent from the reactor was analyzed online using a gas chromatograph (Agilent 7890A) equipped with a 100% dimethylpolysiloxane column (HP-PONA, 50 m \times 0.20 mm \times 0.50 μm) that connected to a flame-ionization detector.

5. Supplementary Tables and Figures

Table S1. Textural and structural properties of the HMOR samples.

Sample	$\text{SiO}_2/\text{Al}_2\text{O}_3^{\text{a}}$	$\text{SiO}_2/\text{Al}_2\text{O}_3^{\text{b}}$	$\text{Al}_{\text{ex}}\%^{\text{c}}$	S_{BET} (m^2/g)	S_{micro} (m^2/g)	V_{total} (cm^3/g)	V_{micro} (cm^3/g)	NH_3 (mmol/g) ^d		
								8-MR	12-MR	Total
Nanosheets	27.0	35.4	15.6	364	303	0.30	0.12	0.80	0.30	1.10
Micro-sized	29.8	30.2	10.5	478	377	0.29	0.15	0.81	0.12	0.93

^aMeasured by ICP-OES; ^bMeasured by ^{29}Si NMR spectra; ^cExtra-framework alumina, measured by ^{27}Al NMR spectra; ^dMeasured by NH_3 -TPD profiles.

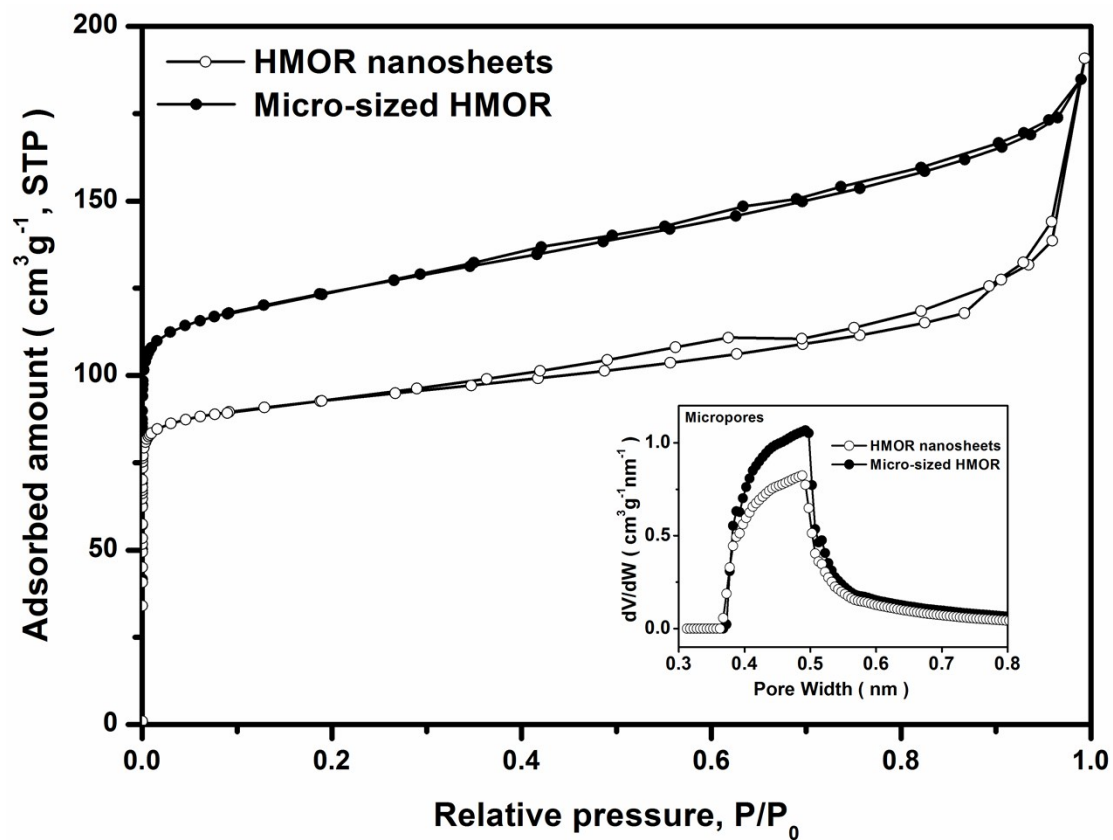


Fig. S1 Nitrogen adsorption-desorption isotherms and micropore size distribution (inset) of the HMOR nanosheets and the micro-sized HMOR.

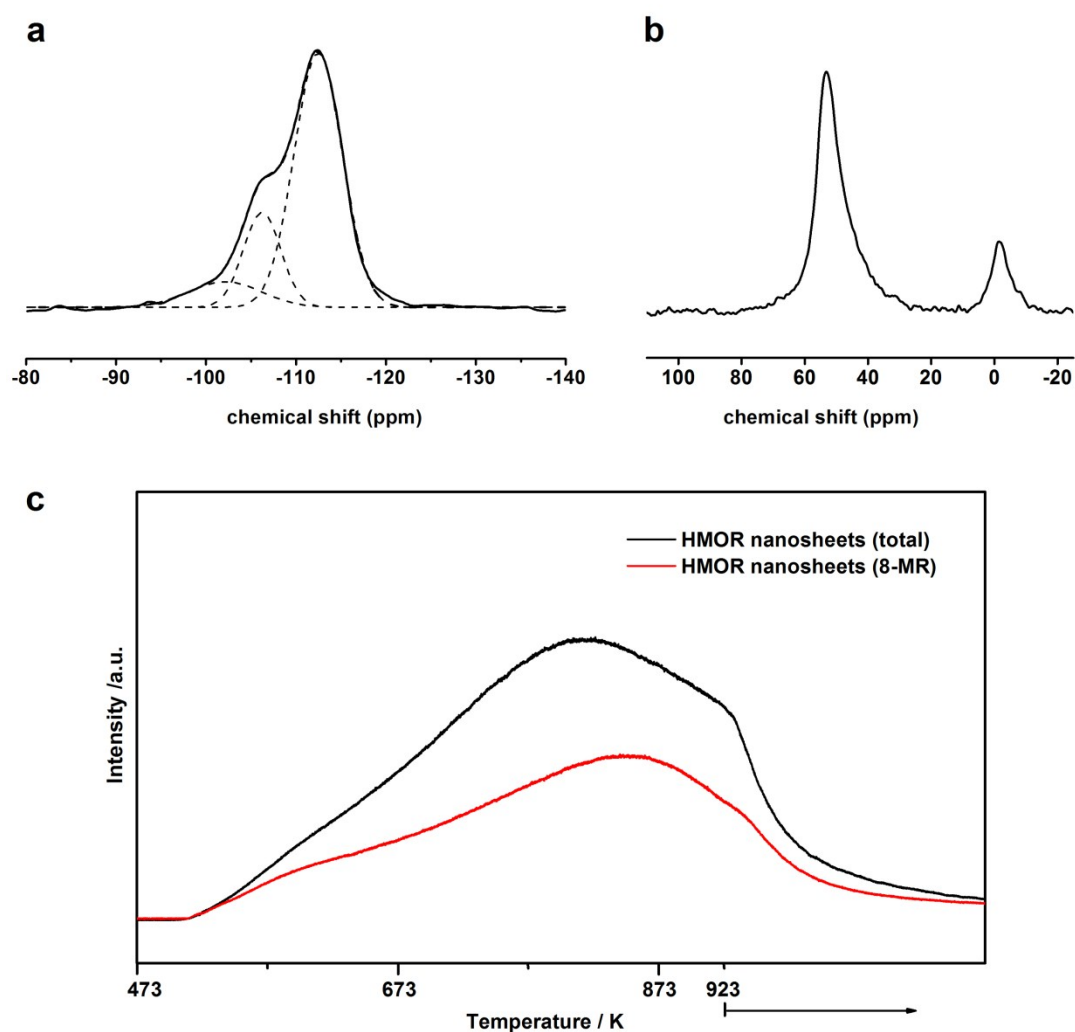


Fig. S2 ^{29}Si MAS NMR spectrum (a) and ^{27}Al MAS NMR spectrum (b) and NH_3 -TPD profiles (c) of the HMOR nanosheets. The ^{29}Si MAS NMR spectrum consisted of Si(OAl), Si(1Al) and Si-OH units with chemical shifts at -113 , -106 , and -103 ppm, respectively.³ The peaks in the ^{27}Al MAS NMR spectrum at 54 ppm and 0 ppm represented tetrahedrally (Al^{IV} , 84.4%) and octahedrally (Al^{VI} , 15.6%) coordinated aluminum species, being ascribed to framework and extra-framework aluminum species, respectively.⁴ The amount of acid sites in the 12-MR channels was calculated from the total acid sites after subtracting acid sites in the 8-MR pores (8-MR channel and side-pockets). The amount of acid sites in the 8-MR pores was measured by pre-adsorption of pyridine in the 12-MR channels.^{2, 5}

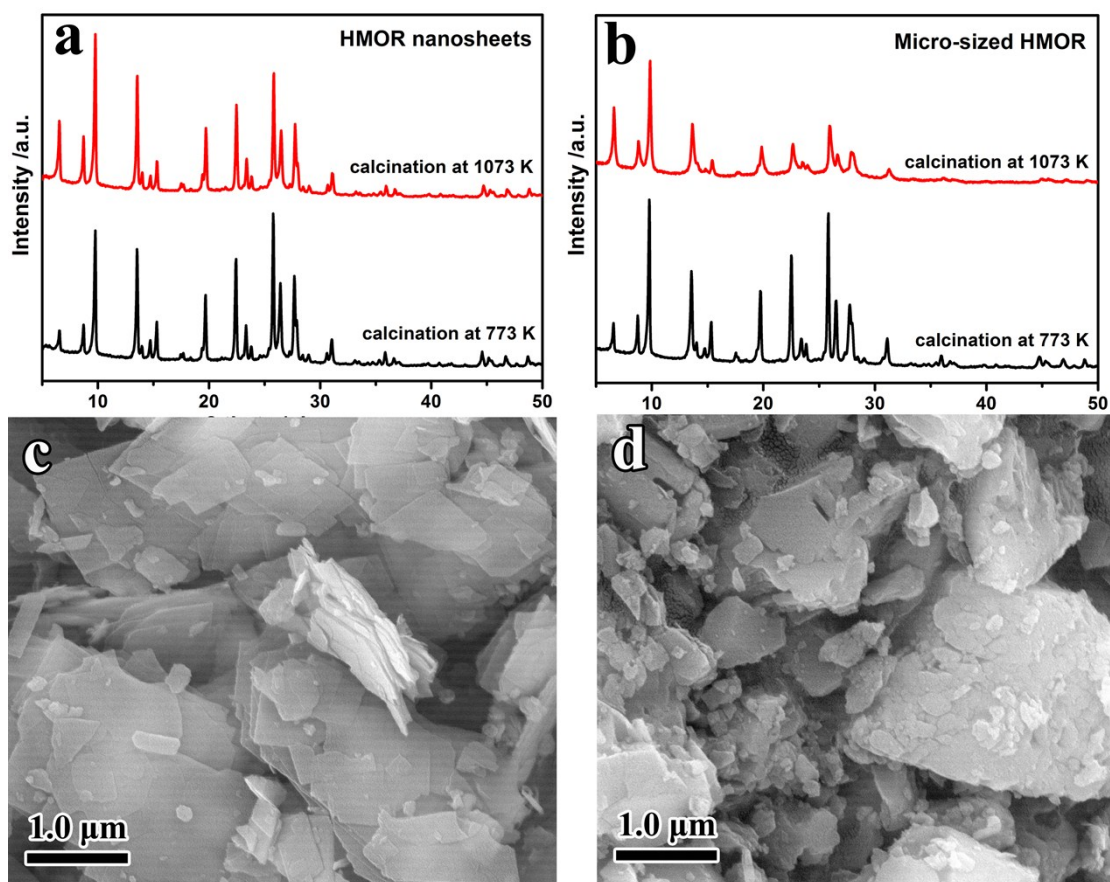


Fig. S3 XRD patterns and SEM images of the HMOR nanosheets (a, c) and the micro-sized HMOR (b, d) after calcination at 1073 K in air for 2 h (XRD patterns of samples after calcination at 773 K were shown for comparison).

After calcination at 1073 K in air for 2 h, the HMOR nanosheets contained small amount of irregular particles, but the relative crystallinity slightly increased to 105% as compared with the typical sample that was calcined at 773 K (the crystallinity was calculated by integrating the area of the peaks at 2theta of 5-28° in the XRD patterns). For the micro-sized HMOR after calcination at 1073 K, more irregular particles were formed and the relative crystallinity decreased dramatically when compared with the sample calcined at 773 K (Fig. S7).

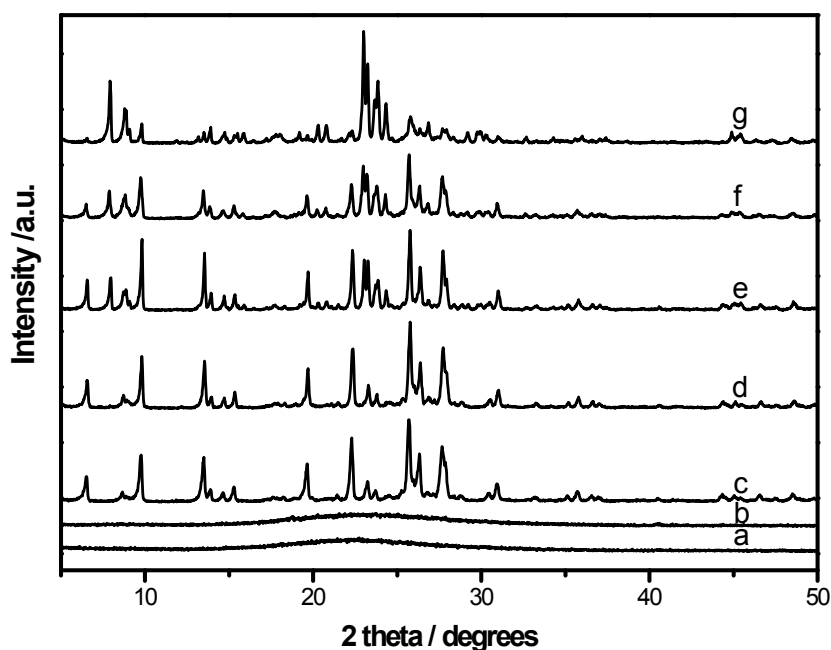


Fig. S4 XRD patterns of the MOR samples synthesized by varying the $\text{SiO}_2/\text{Al}_2\text{O}_3$ ratio in the initial gel: (a) 10, (b) 15, (c) 25, (d) 30, (e) 35, (f) 40 and (g) 50. The samples were hydrothermally treated at 423 K for 6 days. At high $\text{SiO}_2/\text{Al}_2\text{O}_3$ molar ratios (35-50), the products contained mixed MOR and ZSM-5 phases.

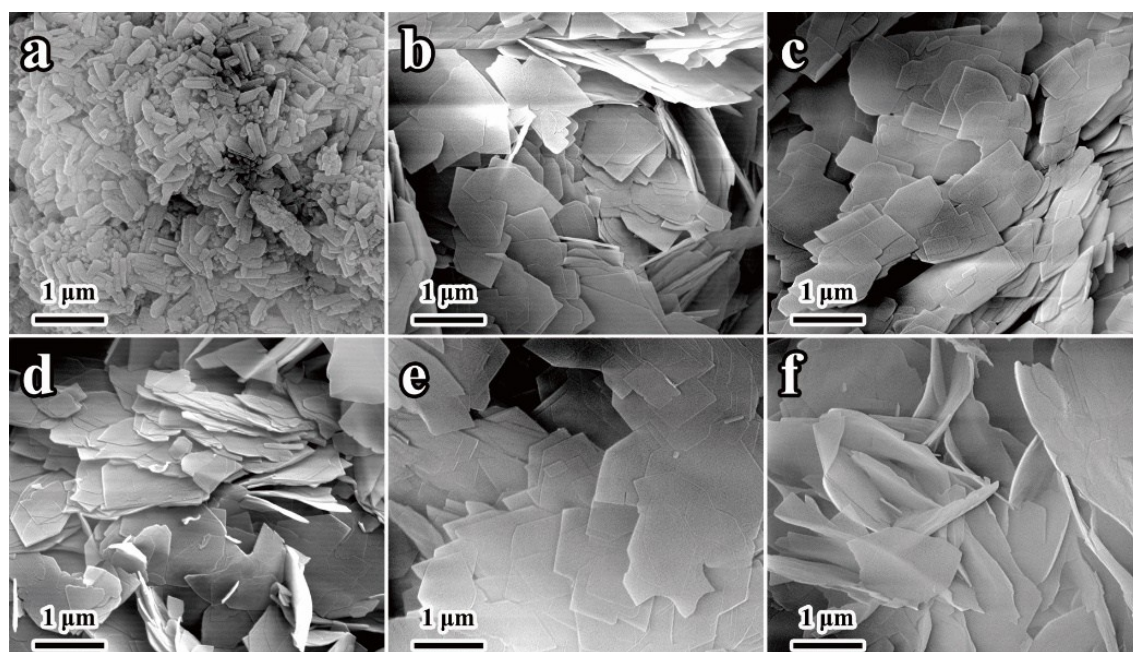


Fig. S5 SEM images of the MOR samples synthesized with varying the $\text{SiO}_2/\text{Al}_2\text{O}_3$ ratio in the initial gel: (a) 20, (b) 25, (c) 30, (d) 35, (e) 40 and (f) 50. The samples were hydrothermally treated at 423 K for 6 days. The morphology of the product was prism-like at the $\text{SiO}_2/\text{Al}_2\text{O}_3$ ratio of 20 (a) and it shifted to sheet-like as the $\text{SiO}_2/\text{Al}_2\text{O}_3$ ratio increased to 25-50 (b-f).

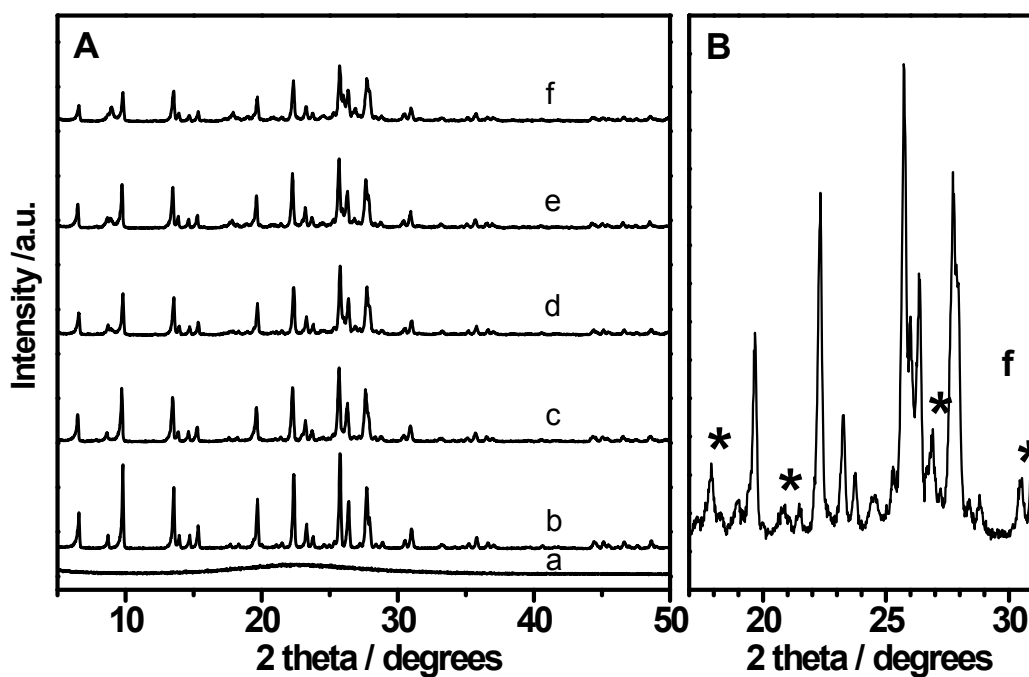


Fig. S6 (A) XRD patterns of the samples obtained during the hydrothermal synthesis under the optimal conditions at (a) 0, (b) 2, (c) 4, (d) 6, (e) 8 and (f) 10 days. (B) enlarged XRD pattern of the sample obtained after hydrothermal synthesis for 10 days, showing the presence of silicon oxide phase. The hydrothermal synthesis was performed at 423 K with the initial gel composition of 8.4 Na₂O:1.0 Al₂O₃:30 SiO₂:1260 H₂O:120 EtOH:1.2 C₁₆₋₂₋₀.

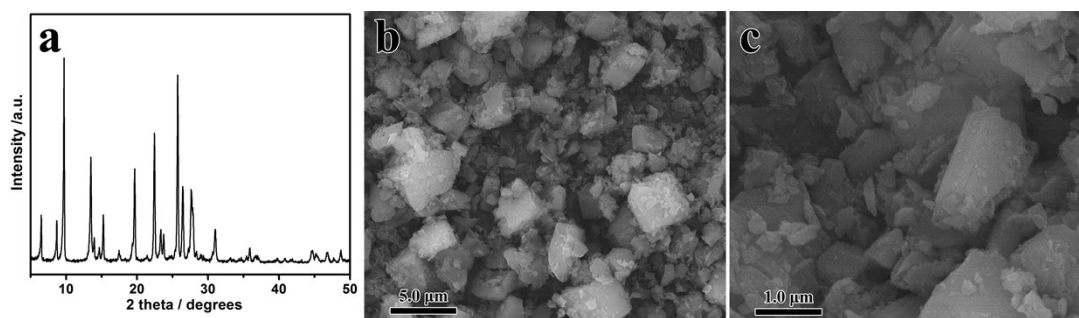


Fig. S7 XRD pattern (a) and SEM images (b-c) of the micro-sized HMOR.

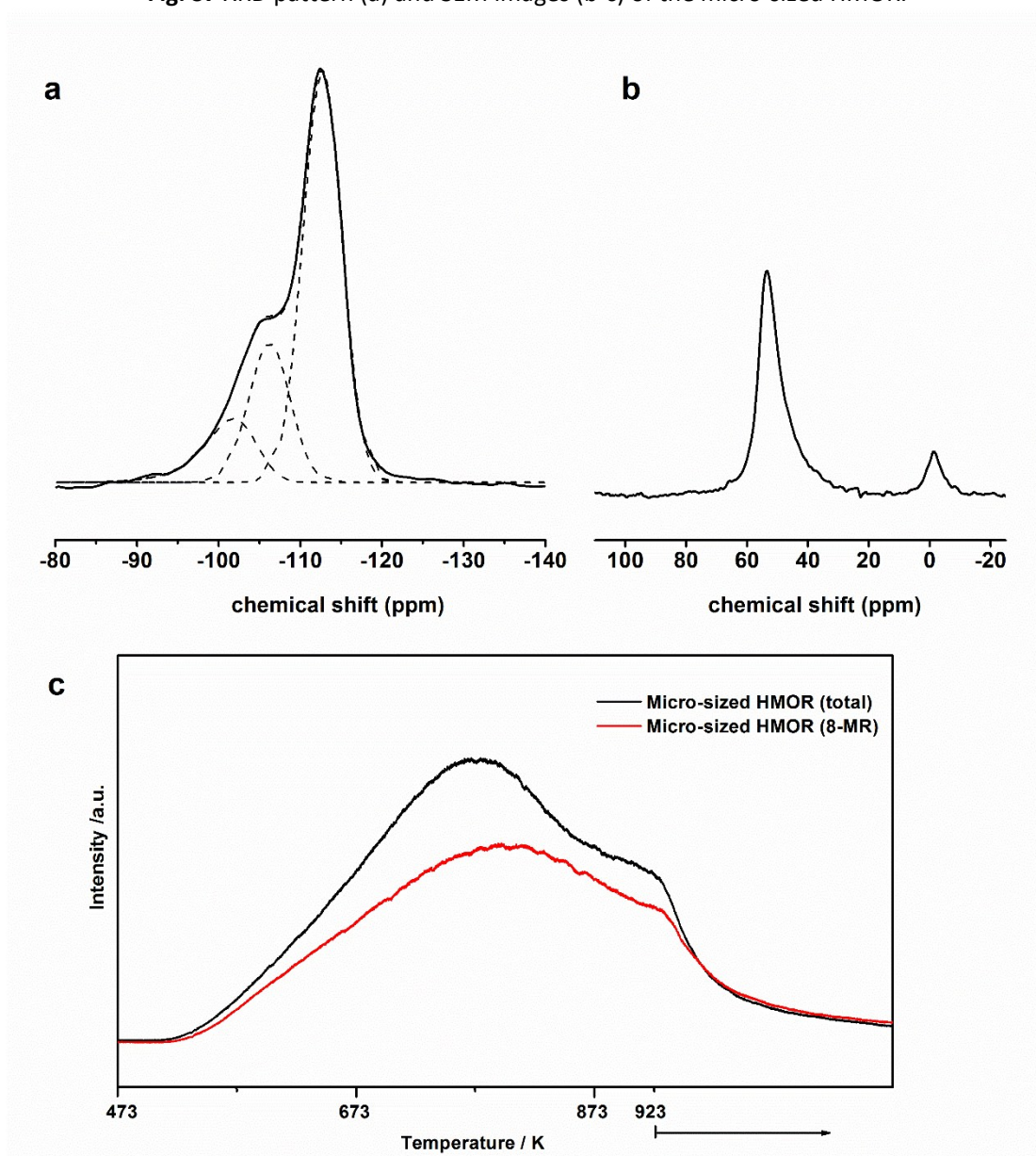


Fig. S8 ^{29}Si MAS NMR spectrum (a) and ^{27}Al MAS NMR spectrum (b) and NH_3 -TPD profiles (c) of the micro-sized HMOR. Judged from the NH_3 -TPD and NMR profiles, the micro-sized HMOR had almost the same amount of acid sites in 8-MR pores and about half amount of acid sites in 12-MR channels, as compared with the HMOR nanosheets (Fig. S2).

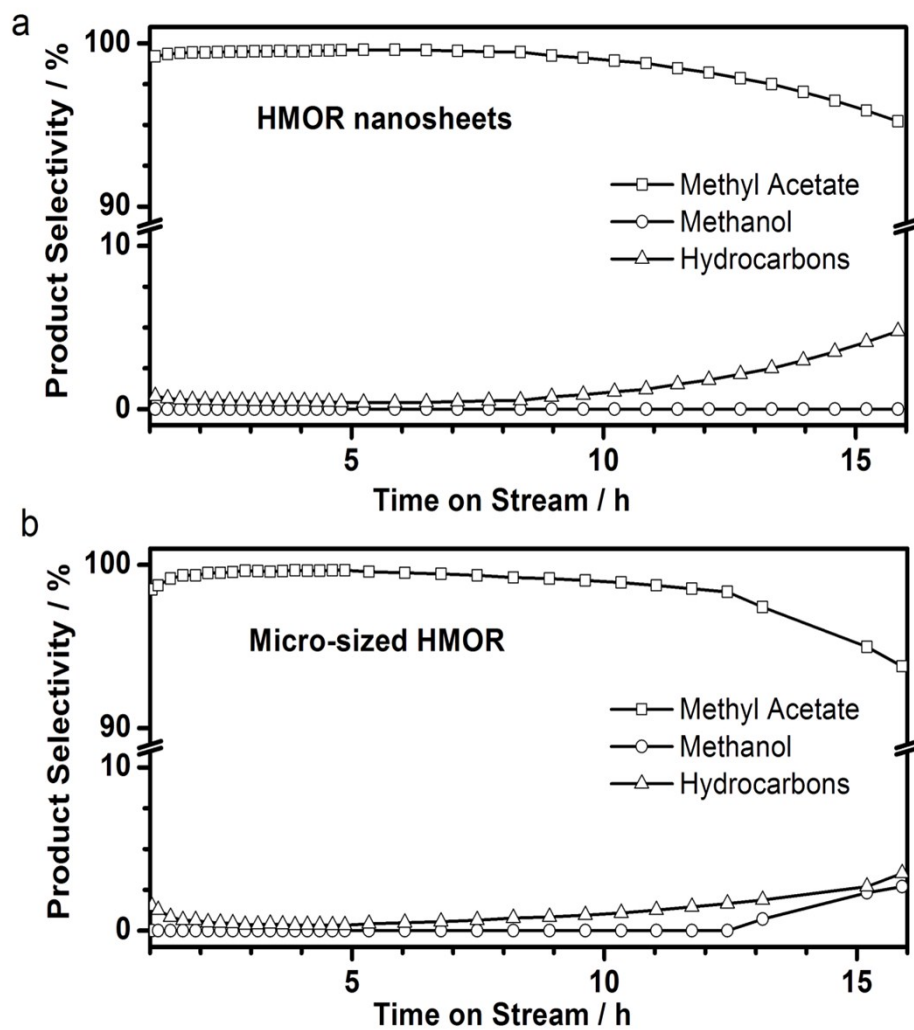


Fig. S9 Product selectivity of DME carbonylation over the HMOR nanosheets (a) and the micro-sized HMOR (b) as a function of time on-stream. Both samples showed quite similar product distributions. 473 K, 1.0 MPa, DME/CO/N₂/He=5/50/2.5/42.5 (vol.%), 1250 mL/(g·h).

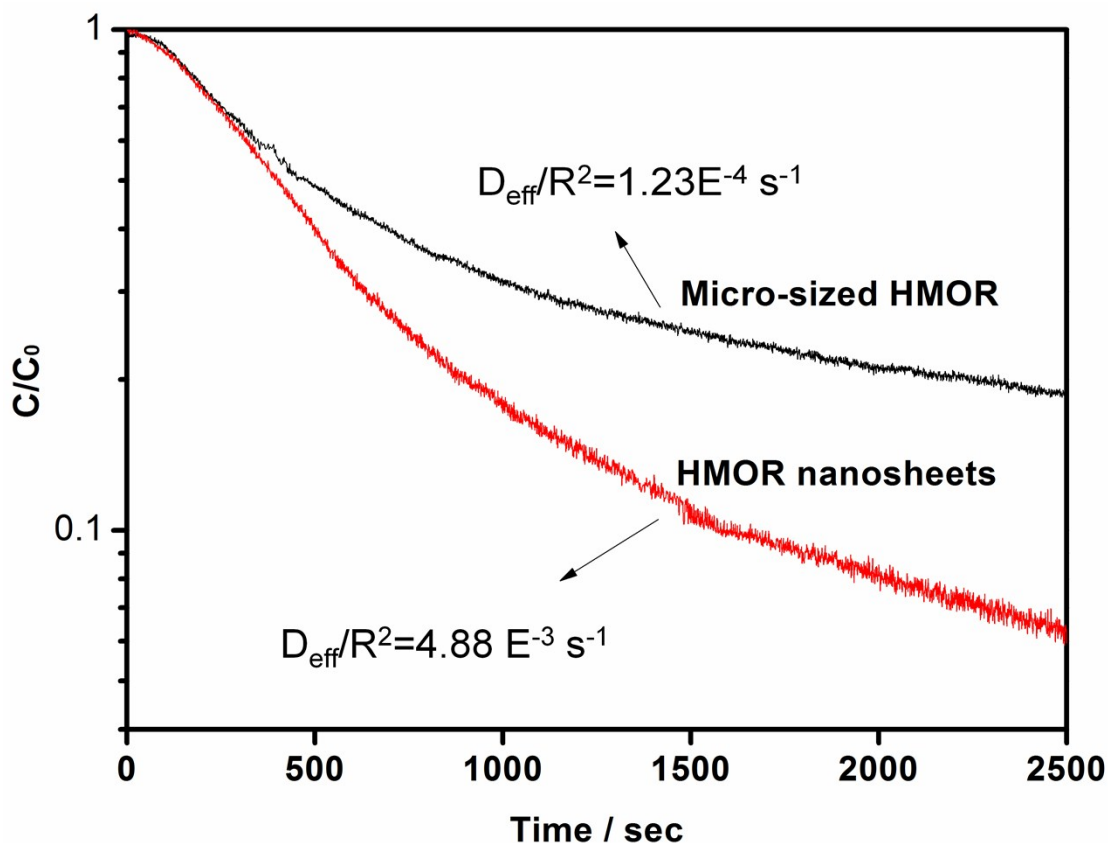


Fig. S10 ZLC desorption curves of toluene on the HMOR nanosheets and micro-sized HMOR. The result showed that the effective diffusion constants (D_{eff}/R^2) of toluene on the HMOR nanosheets ($4.88\text{E}^{-3}\text{ s}^{-1}$) was much higher than that on the micro-sized HMOR ($1.23\text{E}^{-4}\text{ s}^{-1}$), demonstrating the significantly shortened diffusion length in the HMOR nanosheets. The diffusion behavior of toluene on the HMOR samples was measured by the zero length column (ZLC) method.⁶⁻⁹ 20 mg sample was loaded into the ZLC column (3 mm diameter) and treated at 543 K for 4 h in a helium flow (15 mL/min) to eliminate possible impurities and moistures. The sample was then equilibrated with toluene (0.33 vol.%) diluted by helium at 313 K. Desorption was performed by purging the samples with helium (30 mL/min). The concentration of the toluene in the effluent was monitored by a mass spectrometry (Omnistar QMS200).

References

- 1 H. F. Xue, X. M. Huang, E. Ditzel, E. S. Zhan, M. Ma and W. J. Shen, *Ind. Eng. Chem. Res.*, 2013, **52**, 11510-11515.
- 2 H. F. Xue, X. M. Huang, E. S. Zhan, M. Ma and W. J. Shen, *Catal. Commun.*, 2013, **37**, 75-79.
- 3 J. Barras, J. Klinowski and D. W. McComb, *J. Chem. Soc., Faraday Trans.*, 1994, **90**, 3719-3723.
- 4 X. F. Li, R. Prins and J. A. van Bokhoven, *J. Catal.*, 2009, **262**, 257-265.
- 5 R. Buzzoni, S. Bordiga, G. Ricchiardi, C. Lamberti, A. Zecchina and G. Bellussi, *Langmuir.*, 1996, **12**, 930-940.
- 6 E. Mangano, S. Brandani and D. M. Ruthven, *Chem. Ing. Tech.*, 2013, **85**, 1714-1718.
- 7 V. T. Hoang, Q. L. Huang, A. Malekian, M. Eic, T. O. Do and S. Kaliaguine, *Adsorption.*, 2005, **11**, 421-426.
- 8 L. Huang, Q. Huang, H. Xiao and M. Eic, *Microporous Mesoporous Mater.*, 2008, **114**, 121-128.
- 9 H. Zhao, J. Ma, Q. Zhang, Z. Liu and R. Li, *Ind. Eng. Chem. Res.*, 2014, **53**, 13810-13819.